LAWRENCE
LIVERMORE
NATIONAL
LABORATORY

UCRL-JRNL-200955

Design Integration of Liquid Surface Divertors

R. E. Nygren, D. F. Cowgill, M. A. Ulrickson, B. E. Nelson, P. J. Fogarty, T. D. Rognlien, M. E. Rensink, A. Hassanein, S. S. Smolentsev, M. Kotschenreuther

November 14, 2003

Fusion Engineering and Design

UCRL-JRNL-200955

Design Integration of Liquid Surface Divertors

R.E. Nygren, D. F. Cowgill and M.A. Ulrickson, Sandia National Laboratories[1]
B.E. Nelson and P.J. Fogarty, Oak Ridge National Laboratory
T.D. Rognlien and M.E. Rensink, Lawrence Livermore National Laboratory
A. Hassanein, Argonne National Laboratory
S.S. Smolentsev, University of California, Los Angeles
M. Kotschenreuther, University of Texas, Austin

Abstract

The US Enabling Technology Program in fusion is investigating the use of free flowing liquid surfaces facing the plasma. We have been studying the issues in integrating a liquid surface divertor into a configuration based upon an advanced tokamak, specifically the ARIES-RS configuration. The simplest form of such a divertor is to extend the flow of the liquid first wall into the divertor and thereby avoid introducing additional fluid streams. In this case, one can modify the flow above the divertor to enhance thermal mixing. For divertors with flowing liquid metals (or other electrically conductive fluids) MHD (magneto-hydrodynamics) effects are a major concern and can produce forces that redirect flow and suppress turbulence. An evaluation of Flibe (a molten salt) as a working fluid was done to assess a case in which the MHD forces could be largely neglected. Initial studies indicate that, for a tokamak with high power density, an integrated Flibe first wall and divertor does not seem workable. We have continued work with molten salts and replaced Flibe with Flinabe, a mixture of lithium and sodium fluorides, that has some potential because of its lower melting temperature. Sn and Sn-Li have also been considered, and the initial evaluations on heat removal with minimal plasma contamination show promise, although the complicated 3-D MHD flows cannot yet be fully modeled. Particle pumping in these design concepts is accomplished by conventional means (ports and pumps). However, trapping of hydrogen in these flowing liquids seems plausible and novel concepts for entrapping helium are also being studied.

[1] Sandia is a multi-program laboratory operated by Sandia Corporation, a Lockheed Martin Company, for the NNSA United States Department of Energy under Contract DE-AC04-94AL85000.

1 Introduction

The goal of identifying an attractive path for the commercialization of fusion energy has prompted research on the design of fusion chambers with high power density and liquid wall facing the plasma. Lower cost for electricity is associated with the goal of high power density. Liquid walls offer various potential benefits, such as simplifications in remote handling, the flexibility of an automatically regenerated surface and its robustness against temporary local overheating, and lower recycling at the plasma edge,

With high power density comes a corresponding challenge that,very high power originating as the kinetic energy for particles must be exhausted from the core plasma. If this proceeded without mitigation, the heat flux onto a target plate orthogonal to the separatrix would be several Gigawatts per square meter. Thus a fundamental goal in toroidally-confined high power density concepts,is that a large fraction (>90%) of the particle power must be converted into (EM) radiation in the core or edge plasmas so that the power carried onto the divertor targets by charged particles is manageable.

With liquid surfaces comes the challenge of a radical departure in both conception and technology from the current as well as the next generation of fusion experiments. Fusion chamber designs with liquid surfaces are being explored in the APEX (Advanced Power Extraction) Program[1], and work on liquid surface plasma facing components and related plasma surface interactions is being performed in the Advanced Limiter-Divertor Plasma Facing Systems (ALPS) Program.[2] There is also directed effort (called "ALIST") on the future deployment of a liquid surface module in NSTX that draws upon the resources in ALPS and APEX.[2] Within the scope of APEX, which includes for example, the development of MHD models and experiments for liquid metal flows, is a task in which we identify and solve the practical engineering issues associated with liquid surface plasma chambers, including divertors.

Interest in liquid surface divertors certainly did not begin with the APEX. The need to use Li to breed tritium for D-T fusion reactors led to the possibility of using liquid Li in the chambers. The excellent heat transfer of liquid metals is well known. Applications include heat pipes and liquid metal fast breeder reactors. Liquid divertor designs with flowing films, jets, droplets and solid walls wetted have been proposed[3-23], and a gallium divertor was tested in the Russian T-10 tokamak.

1.1 APEX Chamber Design

Our divertor designs to date in APEX have adapted the configuration of ARIES-RS[3][24,25] to incorporate a liquid surface first wall and divertor and a liquid blanket. but have specified a higher fusion power of 3840MW, alpha power of 767MW and auxiliary power of 142MW to define the heat loads for the first wall and divertor. In preliminary evaluations of the first wall (FW) and blanket, a concept proposed by Neil Morley of UCLA with separated streams of flowing

[2] Information can be found on the ALPS website <http://www.td.anl.gov/ALPS_Info_Center>

[3] ARIES-RS is a 2170MW D/T conceptual power plant design with 16 TF coils, a major radius of 5.5m, an aspect ratio of 4, a plasma current of 11MA and a density of $2x10^{20}m^{-3}$. The alpha power is 433MW and the total power to be exhausted into the scrape-off layer or (and) radiated is 532MW.[24] These values were slightly amended in a later paper[25] that discussed the ARIES-RS divertor and described its strongly radiating feature.

liquid for the FW and blanket was deemed the most promising. A 2-cm thick FW stream is the immediate physical boundary outside the plasma. Behind the first wall is a slower flowing liquid blanket of Flibe or Li-Pb.

In the simplest implementation, the first wall flow in the chamber becomes the divertor flow at the bottom of the machine. Introducing a separate divertor stream could have the potential advantages of separate control for fluid parameters such as inlet velocity and temperature but also adds the complexity of a separate flow loop. This paper summarizes the various aspects of the current design and focuses on work to design a divertor with extended flow from the FW.

1.2 Design History

Our mechanical design has proceeded through several design concepts and each has included detailed CAD renderings and several innovative features. One example is a system of nozzles that launch the first wall flow. The nozzles are "self shielding" in that the flows overlap in a way that prevents line of sight from the plasma to the solid surface of a nozzle. Another innovation was a flexible "bag" of SiC used to guide the blanket flow stream and separate this from the flowing first wall. The temperatures of the flow streams are consistent with requirements for efficient power generation. The design effort has included an evaluation of safety concerns and state-of-the-art modeling, such as the modeling of the plasma edge, done within the APEX and ALPS Programs. These innovations and information on safety are included in an overview paper on our design work[26] and in several other papers in this issue of Fusion Engineering and Design. Also, we remind readers that this paper is more a progress report than a design summary since our work continues and some aspects are not yet done.

The development of our chamber designs has included designs with Li, Flibe, Sn or Ga, and most recently, Flinabe, as candidates evaluated for the first wall and divertor stream. Fig. 1 shows the path of our liquid surface chamber designs and some of our preliminary conclusions.

In 1999 and early 2000, we studied Li and Flibe. Both had problems with limited windows for operating temperature. Excessive surface temperature (vaporization of F) limited the Flibe design, and poor thermal efficiency limited the Li design. Sn-Li was also evaluated with the hope that the lower activity of the Li in the mixture and lower evaporation rate would raise the allowable surface temperature of the first wall for operation. The increase was a significant, from 380°C for Li to 590°C for 0.8Sn-0.2Li[27]. The phenomenon of segregation of Li to the surface was also identified, and the potential benefit of having a renewable lithium-coated tin surface was noted.[28]

In 2000 and 2001 we began evaluating designs with Sn. The analysis of plasma surface interactions gave a fairly good operating temperature range with the surface temperature limit of Sn in the ARIES/CLIFF design being 810-840°C for the FW and 1630°C (1480°C for Ga) for the divertor. (References are given later.) However, accurate evaluations of the fluid flows, particularly for the

divertor, were not yet available due to the difficulty of modeling the complications arising from liquid metal magneto-hydrodynamic (MHD) effects. To our knowledge the MHD issues have not been definitively addressed in any proposed fusion reactor designs to date where high power density is desired. MHD issues are discussed in another paper in this journal.[29]

In FY2002 we began evaluating the salt, Flinabe, which is a mixture of lithium and sodium fluorides and has similarities to Flibe but with a lower melting point (an issue still in question). While the MHD effects found with liquid metals can be largely mitigated by using molten salts, these salts typically have poor thermal conductivity. We evaluated Flibe and then Flinabe to study the possible benefit of heat dissipation in turbulent flow. The Flinabe design is the main subject in this paper. The issues and R&D needs are included in another paper[26] that presents an overview of the Flinabe design.

2 Particle Handling and Plasma Edge Modeling

In our liquid surface designs, we presume vaporization from the liquid surfaces to be the primary source of plasma impurities. Since the vaporization rate is exponentially dependent upon temperature, there is a narrow range in which the impurity generation rate changes from low to unacceptable.

Plasma edge modeling by authors Rognlien and Rensink[27,29,30] with the 2D UEDGE code provides particle loads and the power deposition profiles in the ARIES/CLIFF divertor. Early modeling was done with the results for a double null divertor but subsequently a single null model was developed. The UEDGE modeling is complemented by that of Brooks using the BPHI-3D code, a sheath model with 3-D capability[31-33], to evaluate effects within the plasma sheath at the divertor and the WBC code for near-surface transport of sputtered impurities[34].

This modeling work also makes use of theoretical and experimental research on the physical response of liquid surfaces that affect their sputtering, erosion and redeposition that will not be covered in any detail here. The effect of Li surface segregation[28] was mentioned previously. Other examples are the apparent increase in sputtering yields of metals in the liquid state as compared with the solid state[35,36], and various studies on sputtering yields and trapping[37-40].

2.1 Edge Modeling with Li or Flibe Walls

The modeling has dealt with several aspects of the plasma edge that differ from more conventional machine operations, where measurements are also available to compare with the modeling. Ref. [27] describes early efforts in modeling Li walls in which the Li is assumed to be an active sink for hydrogen and severely reduces the recycling at the edge. For Li, the maximum fluid temperature limit based on a threshold level for the Li core impurity level in the model was about 380C for a low R_H of 0.25. The criterion for the maximum acceptable impurity level was that T_e at the wall collapsed and the solution was not stable for higher impurity influxes. Here the range of coolant temperature was judged to be too low for high efficiency in power generation; this conclusion was also tied to other analysis regarding a flowing Li blanket.

In subsequent work, authors Rognlien and Rensink[30] studied the penetration into the plasma of F, the most dangerous core-contamination component of Flibe. For a flow of 10m/s, the transit time for flow down the ~6m poloidal length of the first wall is 0.6s. Although there is a rise in temperature from top to bottom, authors Rognlien and Rensink have shown the rate of impurity generation for the first wall can be fairly well estimated by using the average first wall temperature in calculating the impurity source. For the first wall, the dominant effect in impurity generation is its very large area. Also, for a molecular coolant, such as Flibe or Flinabe, there is the complication that the subsequent breakup of evaporated molecules can produce neutrals with velocities much greater than those associated with evaporation. This modeling shows that, with high hydrogen recycling (R_H=0.98) and without some scheme other than simple pumping to enhance impurity removal at the edge, impurity contamination from Flibe would be problematic down to its melting point. (This modeling was done for an ITER divertor, selected because there is more documentation than for ARIES.) While some ideas for dealing with the edge impurities were advanced (e.g., heating the edge to mitigate radiation), effort on design was redirected to other fluids.

2.2 Edge Modeling with Sn or Ga Walls

The Sn first wall and divertor appear in our initial evaluations to have a workable range in the fluid temperatures to make an attractive design. The type of modeling for the first wall mentioned above has also been done for Sn but a paper summarizing this work has not yet been published This yielded a maximum allowable temperature for a Sn first wall of 735°C for an R_H of 0.99. (A fairly high radiated fraction, f_{rad}, of 0.87 was assumed to reduce the power load to the divertor, although a specific technique for achieving this was not included at that time in the design.) For a similar case, but with an f_{rad} of 0.74, the peak power rose to about 55MW/m^2. Power deposition profiles from the modeling were used for evaluation of the thermal performance of the divertor as described later. Figure 2 shows the limits for operating temperatures based on limits for impurity generation obtained from the edge modeling for our initial studies.

With regard to the maximum allowable surface temperature in a Sn divertor, this temperature can be higher temperature than for the first wall since a more difficult path is anticipated for impurities from the divertor to come back into the core plasma than for impurities from the first wall. In the specific case of thermal impurities launched by vaporization, only a tiny fraction of the atoms ever escape the sheath, i.e., the mean free path for ionization of the slow evaporated Sn atoms is small compared to the thickness of the sheath. Table 1 shows results of sheath modeling for evaporated Sn for typical “high recycling” divertor conditions, Here a less rigorous treatment than the full 3-D power of the code is used; for example, lateral gradients in surface temperature and plasma properties are ignored and the surface is presumed to be of uniform temperature. The criterion is that the solution must be stable for a time equal to the time it takes the flowing liquid to pass through the strike zone of the divertor, typically a few milliseconds for a fluid flowing at 10m/s.

Using the results above and extrapolation from sheath/thermal studies[31-33], Brooks estimates that a large local vaporization rate of Sn at the surface of the liquid, equal to ~20% of the incoming DT particle flux, still results in an acceptable level of Sn escaping from the sheath, which is the critical impurity source term at the plasma boundary above the sheath. This limit corresponds to the evaporation rate (and thermal velocity) of Sn at ~1300°C. Also estimated is a rough "allowable value" of ~1630°C for the maximum temperature of a "hot spot" with a 1cm diameter. This even higher temperature in a hot spot is permissible with respect to impurity generation because the area generating impurities at a much higher rate is small.

2.3 Edge Modeling with High Radiation

Radiating a high fraction of the particle power is essential for the design approaches described here, as noted earlier. In the ARIES design study[25], radiation from “highly radiating rings” in the inboard and outboard divertors reduced the direct heat load from particles onto the strike points of the divertors. Recent and as yet unpublished work for ALPS and APEX by Rognlien and Rensink on Flinabe gives significant support for the hope that stable plasmas can be produced with a large amount of power convected from the core to the edge and highly radiating regions of edge plasma . (A limitation is that the edge model does not include a self-consistent core transport). These recent results show steady state modeling solutions in which about 95% of the power coming into the scrape-off layer is radiated near the X-point for alpha powers in the range of 300-360MW.

Figure 3 shows the UEDGE mesh for the ARIES/CLIFF model and Figure 4 shows the heat load from radiation on the first wall and divertor from the UEDGE code for the Flinabe chamber design. The horizontal axis in Figure 4 is the length along the outer boundary in the UEDGE model that represents the free surface of the fluid. This path starts at the bottom of the inner divertor surface, goes up the surface of the inner first wall and then down the surface of the outer first wall and down the surface of the outer divertor. The peaks at the left and right are the higher heat loads on the inner and outer divertors, respectively. The radiative heat-load shown in Figure 4 is what heats the surface of the liquid as it flows through the chamber and gives rise to the evaporative flux of fluorine vapor. An iterative procedure is used to obtain the surface temperature consistent with the edge plasma conditions

Figure 5 shows this key result of a highly radiating edge plasma with plots the fluorine radiation density in four modeling cases and increasing amounts of alpha power. The parameter, P_c, in the figure is the power convected from the plasma core to the edge plasma. Most of this power is radiated so that the remaining power carried as particles to the divertor target results in a manageable peak heat load. In the first case (a), there is limited radiation in the zones near the X-point and the solution is unstable (MARFE). The second and third cases (b and c) are stable and radiate strongly. The fourth case (d) is unstable and the hot plasma edge “burns through” to convect an unacceptably large heat load to the

surface of the divertor. These are detached plasmas with high densities, high recycling and very low throughput (exhaust) of particles.

The condition for 300MW produced a peak heat flux (particle + radiation) at the divertor plate of only ~8 MW/m^2 and a peak heat flux to the first wall of ~2 MW/m^2 for a density at the edge of the core of ~1.5x10^{20} m^{-3}, H (D/T) throughput of ~3.1x10^{23} particles/s with divertor plates orthogonal to magnetic flux surfaces and H pumped at private flux surface for stability. The Fluorine density at core boundary varies poloidally over the range 3.7-7.3x10^{17} m^{-3} (0.24% - 0.49% of hydrogen; 1% is the limit based on core radiation loss). The impurity line radiation is concentrated near the x-point and below, implying a lower maximum surface temperature for the first wall than for (assumed) uniform radiation. The power balance for this case is as follows:

Fluorine radiated power = 223 MW
Hydrogen radiated power = 63 MW (reduced for reabsorption)
Particle power to divertors = 12 MW
Particle power to walls = 2 MW

Figure 5 also shows an additional stable solution with a P_c of 480MW that was achieved later in the design and with different conditions for the Flinabe and the plasma than the other cases. The first set of four cases shows the response of the plasma over a range of values of P_c with stable solutions for a significant subset of this range. Developing the solutions is quite time consuming, and a similar set of cases is not available for the later conditions in our design. However, this latter case, with a stable solution for 480MW of convected power from the core is an extremely pleasing result and corresponds to our “reference” reactor chamber design with flowing Flinabe walls for a high power density fusion, which is described in another paper in this journal.[26]

These results suggest that a highly radiating plasma edge might bring down the divertor heat loads to easily manageable values. An important caveat regarding the plasma edge modeling is that the stability of such highly radiating edge-plasmas. An operating window exists, but outside this window, the edge impurities can either lead to a radiation collapse of the core, or become ineffective in the edge, thereby allowing a large particle heat-flux to reach the divertor. We consider cases where the highly radiating plasma is effective, and this has several implications for our design work. First, the liquid surface does present the potential advantage that this surface is regenerated in the event of a transient that results in excessive local heating that extinguishes the plasma. Second, it is reasonable to investigate designs based upon relatively modest peak heat fluxes (8-10MW/m^2) in the divertor as well as designs in which we maximize the peak heat flux that can be handled.

Certainly there are many unanswered questions and directions of investigation that would be important in advancing the divertor design, for example, the effects of off-normal target angles and the effects of gas puffing at the edge on plasma stability, the distributions of neutrals, etc. Our hope is that advances in the design of power plants and control of plasmas can produce stable plasma

configurations with sufficient radiation from the main plasma and from preferential sites in the plasma edge that the peak power to the divertor can be close to or lower than 10MW/m^2. We believe our preliminary design work suggests that tractable solutions for a divertor with a flowing molten salt could be developed along the lines of the approach reported here.

3 Particle Pumping

Liquid surfaces present several intriguing issues with regard to pumping. Will liquid surfaces pump H or He by trapping the impinging ions (or neutrals)? Although the applications are quite speculative at this time, the underlying ideas do have good scientific bases.

Certainly Li has an affinity for hydrogen. In a reactor with Li walls that strongly pumped D and T (and had very low recycling), one might expect plasma conditions that are much different than in current devices, for example, very high edge temperatures,. This in turn would affect the plasma performance and also the power balance; e.g, the amount of brehmsstralung radiation would increase and also would penetrate further into a Li wall than visible radiation.

There is also the possibility that other liquids may pump He or H through the creation and growth of bubbles as a result of the continuing flux of H or He into the liquid surface. This prospect might lead to designs in which the pumping port used for evacuation of the vessel need not be close to the edge of the plasma.

3.1 Conventional Pumping

For pumping of He, our divertor designs to date still use a conventional approach with exhaust ports and pumps. The initial configuration had lateral ports in the lower portion of the first wall and larger exhaust ducts at the bottom that serve to collect the fluid stream and provide pumping. The current design uses only the bottom ducts for both egress of the first wall and divertor fluid flow and pumping. (See Figs. in Section 3.) Our more recent design also replaces the previous large divertor cassette with a smaller “drawer cassette” for the outboard divertor. This design modification simplified remote handling for the deflector in the outboard divertor and increased the volume of the blanket.

Toroidal breaks in the flow near the bottom of the first wall part the fluid flow and direct it into the opening of the exhaust ducts. The fluid fills only a small portion of the cross section of a duct and the ducts provide adequate total conductance for the modeled D/T throughput and pressure in the divertor of ~3mTorr. The pumping of He was judged adequate based on 2-D modeling of the He density in a high recycling divertor (which we assume for Flibe, Flinabe and liquid Sn) and adequate pumping of the D/T.

Our assertion that the pumping conductance is adequate for a high recycling divertor must be qualified in regard to both the control of pumping and the condition of high recycling. In our current design with liquid Flinabe surfaces, a plasma edge modeling solution for the desired power balance has been achieved without the use of gas puffing at the edges and with high recycling and very low throughput. We can anticipate that such a solution might be sensitive to “excess

pumping" in the divertor. Without significant gas puffing, some control of the pumping might be achieved through the use of baffles. A better estimate of the pumping could be obtained with a Monte Carlo calculation for our divertor configuration and a specified plasma edge condition. Since this is the n^{th}–of-a-kind power plant, we assume that the proper pumping balance has been achieved.

With Flinabe as the surface interacting with the plasma, we are assuming that there will be little retention of either implanted helium or implanted hydrogen (D or T) by the Flinabe. The research on tritium retention in Flibe supports this but the possibility of the entrainment of tiny bubbles formed under high flux bombardment is not well researched.

With other fluids, such as Sn or Sn-Li, we do not yet have plasma edge modeling solutions with the desired power balance between the first wall and divertor and do not have a basis to evaluate the potential issue of helium pumping in such systems. Some interesting work has been done to suggest that helium trapping in liquid metal systems may be possible, but it is premature at this time to apply these results in our design.

3.2 Novel Concepts for Pumping

Some novel ideas for trapping helium in the fluid surface are also being investigated. The notion of trapping helium in a liquid tends to defy the conventional wisdom that one expunges He from solid metals by melting them. Initially there was speculation that, although the diffusion of He out of a fluid surface was rapid, a high flux of He bombarding the fluid in the divertor might build up a large enough He population in the implanted layer that some fraction of the He would remain entrained long enough so that mixing of the fluid in the divertor would bury this entrained He within the fluid and thereby pump it from the chamber. The related calculations for the He in "dynamic" solution under an energetically deposited He fluence indicate that the retained He that could be trapped in solution in the stream would be small unless the implantation energy is higher than we would expect for the edge temperatures in a high recycling divertor and the diffusion of He is slow. However some hope may exist that He release might be slowed if the He were attracted to defects (impurities) or stored in bubbles.

Both experimental work and modeling has been initiated on helium trapping in liquids. Experiments on the trapping of He in a Li stream are being conducted in the FLIRE facility at the University of Illinois.[41] Recent but as yet unpublished works by Hassanien and by Cowgill have been presented at ALPS meetings but are not yet available on the ALPS website.[2]

Hassanien has developed a series of sophisticated codes for the treatment of surface evaporation and ablation and the effects of implanted atoms.[42] He has used the ITMC Code to evaluate the depth profiles of implanted He for various cases and used the HEIGHTS-II code to track the release of this He. For example, in Li with a diffusion of $10^{-5}cm^2/s$, flowing at 10m/s and intercepting

10keV He over 0.2m (Gaussian profile), about 8% of the He would still be retained 0.1m downstream.

Cowgill has applied to several liquid metals a 1-D finite difference diffusion model that accurately describes He nano-bubble formation and growth in solids. The model calculates the binding energy of the n^{th} He atom to a bubble and then evaluates the stability of multiple He groups. Surface tension determines a nano-bubble's stability. The model uses the Stokes-Einstein equation for diffusion of sub-micron particles to evaluate depth concentration profiles for bubbles of various sizes. Mobile He is driven into the liquid if the surface concentrations are high (high incident flux). Coalescence of high concentration small bubbles to form large bubbles is included. The result is He retention that is limited by bubble dissociation rather than by He or bubble migration. He found that there is some tendency for He bubble formation in Li, however it is not large due to the relatively low surface tension, whereas, he found a greater tendency for stable He bubble formation in Ga.

4 Power Handling Issues

The goal of high power density presents challenging engineering, especially for the power handling in a divertor. If, for a constant fusion power, one tries to shrink the chamber (increase the power density), then the divertor heat load increases both because the divertor area gets smaller and because the power scrape-off length diminishes. To mitigate this heat load, one would like to increase the radiated power to the first wall, however, the volume of the plasma edge also decreases as the plasma chamber shrinks. Based on the encouraging results from plasma edge modeling for a Flinabe chamber wall noted in the previous section, we have designed a Flinabe divertor that handles a moderate peak heat load, as will be described.

We also try in our design and heat transfer analysis to understand what would limit the peak power level that can be handled in the divertor. The time for a fluid element at the surface of the divertor to flow across the peaked heat load is only a few milliseconds. The short exposure is the reason that relatively high peak heats loads can be considered with liquid surface divertors.

We are evaluating two classes of coolants, liquid metals (e.g., Li, Sn, Sn-Li or Ga), and molten salts (Flibe and Flinabe). The thermal and electrical conductivities are high for liquid metals and low for the molten salts, and we treat them differently because of their differing physical properties. For example, in our applications, turbulent heat transfer is necessary with molten salts to promote the transfer of heat into the bulk fluid. With liquid metals, most of the heat transfer results from simple conduction.

4.1 Heat Transfer with Liquid Metals

Author Ulrickson made a general assessment (unpublished) of the heat flux limits for flowing liquid surfaces for first walls composed of either Li, Sn75Li25, Sn or Ga; an excerpt is given in the ALPS Report.[43] Based on simple heat conduction without turbulence (slug flow), Ga ranks as the best choice. But there are other factors that impede our evaluation of the liquid metals. For example,

while tin is widely used for soldering in electrical applications, the data on physical properties at temperature much above the melting temperature is rather scant. Another contribution in the ALPS Report indicates some of these limitations in materials data for the liquid metal divertor studies.[44]

For the liquid metals, a major concern is the accurate prediction of MHD-controlled free-surface flows.[4] This affects our design in two ways.

First, MHD forces affect the fluid flow significantly, and 3-D MHD effects will be important, for example, in channeling the flow in the divertor. Modeling MHD-dominated flow in a complicated geometry, such as our divertor, is currently beyond the state-of-the-art. In the ARIES-RS divertor, the field has roughly equal components in the toroidal and poloidal directions and the fluid in the divertor is crossing flux surfaces. Also, the field gradients in the radial direction are important. We placed our work on a Sn divertor "on hold" in 2001 in large part because the capability available for predicting flows in the divertor was insufficient to allow us to design the divertor flow with confidence. From our preliminary considerations of plasma edge interactions and basic power handling, Sn shows promise as a coolant for a single stream first wall and divertor. This is an important conclusion as far as it goes; however, we recognize that the all-important issue of MHD effects on flow has not yet been treated effectively.

Second, we expect MHD effects to suppress classical turbulence. MHD effects tend to force the fluid to flow en masse ("slug flow") like a sliding plate and the heat transfer (oversimplified) is similar to heating a sliding plate from one side. The inherent high thermal conductivity of liquid metals also means the turbulence contributes less in the penetration of heat from the heated surface into the fluid.

Let us compare the heat transfer of a liquid metal to that of water at a velocity of 10m/s in the type of smooth tube of 10mm diameter that we might use for a water-cooled heat sink in a fusion device, i.e., with the heat flux on one side. For water[5] near its maximum (partial nucleate boiling and high sub-cooling), the local heat flux from the wall into the coolant is about 30MW/m^2, the heat transfer coefficient (HTC) is about 0.13MW/m^2-°C (13W/cm^2-°C) and the temperature drop from the wall to the bulk fluid is roughly 230°C. For Li with a thermal conductivity of 44W/m-C and 30MW/m^2 at the liquid metal interface, the HTC is 0.127MW/m^2-°C and the temperature drop across the thermal boundary layer is

[5] The correlations we use have been fitted for data sets where the heat sinks are heated only from one side. The heat transfer coefficient for water is high and increases with heat flux in the regime of partial nucleate heat transfer. With water at a bulk temperature of 50°C (high sub-cooling) and 2MPa and flowing at 10m/s in a 10mm diameter tube, as a tube nears burnout, the local heat flux from the wall into the coolant is about 30W/mm^2 (30MW/m^2 or 3kW/cm^2) and the temperature drop from the wall to the bulk fluid is roughly 225°C.

~236°C based on the treatment by Lyon and Martinelli developed for uniformly heated tubes. [6]

4.2 Heat Transfer with Molten Salts

Our rationale in evaluating a salt as a potential coolant was the possibility that the turbulent heat transfer, i.e., minimal MHD effects due to low its electrical conductivity, would mitigate in part the disadvantage of its low thermal conductivity. Author Smolentsev has modeled the effect of turbulence on heat transfer in Flibe with MHD effects included [45,46] and a sample result is shown later.

Work on the Flinabe divertor is progressing and shows some promise for moderate heat fluxes. The extremely important results of the plasma edge modeling described in Section 2.3 are key in this regard because these solutions indicate that designs with moderate heat fluxes in the divertor may indeed be possible. The latter part of this paper will focus on our recent results with a divertor for the Flinabe chamber design.

There are also still important questions about the basic properties of Flinabe. Is the (assumed) melting point near 300°C really valid? Is the salt a well-mixed single phase fluid in the range of low liquidus temperatures? Work is also in progressing in APEX to address these issues. Reference 26 has more detail on Flinabe.

5 Divertor Configuration and Heat Removal

In developing a divertor configuration, the starting envelope for the mechanical configuration was taken from the ARIES-RS design, and detailed CAD renderings were generated. This work (by authors Nelson and Fogarty) included laying out the envelopes for the flow paths based on a thin flowing first wall stream[7].

Our approach has been to identify design issues as we proceed and specify as much detail as possible while proceeding to develop and improve our conceptual designs. At this point the mechanical features of the divertor include the flow paths and the ducts for pumping and fluid exhaust. For future designs with liquid metals, we anticipate that the exhaust duct at the bottom will include an

[6] Here we use an old treatment by Lyons and Martinelli ($Nu=7+Pe^{0.8}$). With diameter (D), velocity (v), density (□), viscosity (□) and thermal conductivity (k) $Pe=Re*Pr=(Dv□/□)*(C_p□/k)=Dv□/k$. For Sn or Ga, with similar values of thermal conductivity of 33W/m-C, the HTC is about 0.10 nd the temperature drops are about 300°C. Various values of thermal conductivity are reported for Ga and there is little data for Sn at higher temperatures. If we use a much higher value of 58W/m-C for the thermal conductivity of Ga, then the HTC is 0.14 and the temperature drop is only 215°C. We also believe, based on some preliminary comparisons with computational fluid dynamic modeling where the heat removal is handled directly by following the enthalpy and the intrinsically determined HTC is much lower, that the Lyons-Martinelli treatment may not apply well to the case of tubes heated from one side.

[7] Neil Morley and others at UCLA introduced the idea of a thin flowing first wall with a secondary flow stream for the blanket in APEX by their “Concept for a Li Flowing First wall” or CLIFF.

electromagnetic pump to assist in evacuating the liquid metal from the chamber; however little work has yet been done in this area.

In our initial designs for an outboard divertor, the extended FW stream passed through the separatrix before it was deflected downward toward the exhaust duct; as shown in Fig. 6. (This design has the lateral port for RF antennas and a pump duct.)

To increase the peak heat fluxes that could be handled with (turbulent) Flinabe, our more recent divertor design places the flow deflector upstream of the strike point. Now the deflector redirects the outboard flow downward before the flow intercepts the divertor heat flux. Figure 7 shows this revised divertor configuration for the outboard divertor. The 5mm-thick deflector is made of a copper alloy clad in ferritic steel to match other structure. An alternate design is a deflector of advanced (low activation) ferritic steel with internal coolant passages fed by an auxiliary coolant stream that could be exhausted into the divertor.

The location of the deflector upstream of the strike point provides several advantages. First, the deflector modifies the surface layer of the first wall stream and promotes thermal mixing of the previously heated surface layer. Second, the deflector increases turbulence adjacent to its surface. Third, the deflection of the stream above the strike point means that the target angle in the divertor can be manipulated, e.g., a steeper angle spreads out the heat load. Fourth, while the first wall flow can be toroidally continuous across the sector boundaries, the flow in the divertor must be divided into (a minimum of) one separate stream per sector that is directed into the exhaust duct of each of the 16 sectors.

There are two main disadvantages for the upstream location of the deflector. First, misalignment or damage to the deflector may reduce the heat removal capability of the divertor or render it inoperable. Second, the deflector is a solid component that directly faces the plasma in a position that probably presents a greater risk of generating impurities that would affect plasma performance that the downstream location (in the private flux region). The impurity generation from the solid surface of the deflector has not yet been included in the plasma edge modeling.

5.1 Divertor Heat Removal

In evaluating the heat removal in the divertor, we use the heat distribution from the plasma edge modeling described in Section 2 and apply this to the surface of the flowing liquid in the divertor. Figure 8 shows the heat distribution from the UEDGE model (similar to Fig. 4) for a case in which the radiation from the plasma core and plasma edge is sufficient to produce a peak heat load of only 10-12MW/m^2 for the case of a single null Flinabe divertor. Also (added) in the figure is an approximated flat profile with a peak heat flux of 10.6MW/m^2 that is the sum of the uniform radiated heat flux into the divertor of ~3 MW/m^2 plus the average of 7.6 MW/m^2 over the peak.

Since the fluid passes rapidly across the region of peak heat flux and the time for heat penetration is only a few milliseconds, this is a transient heat conduction

process (both conduction and capacitance parts in solving the Fourier equation), i.e., the heat penetrating the surface is first being absorbed into the heat capacity of the thermal boundary layer as the thermal gradient develops and then conducted deeper into the stream. Although there is some bulk heat generation from nuclear heating it is insignificant in the divertor heat transfer.

Author Smolentsev has calculated the temperature rise in the divertor for this heat load and a Flinabe stream entering at 420ºC and flowing at 10m/s. Figure 9 shows the results. The temperature rises rapidly within a short distance due to the high heat flux and generally poor thermal conductivity of the Flinabe. The rise in temperature is about 135ºC. This, added to the bulk temperature of 420ºC leaving the first wall, gives a peak of about 555ºC. This is higher than the allowable temperature of 510ºC for the first wall, but is acceptable in the divertor where there is more shielding of impurities from the main plasma. Additional analysis of the divertor heat transfer appears in the next section.

Author Smolentsev uses an approach based on the standard "K-_" model to characterize turbulent flow and has developed a heat transfer model that includes MHD (magneto-hydrodynamic) effects. Typical output includes the flow thickness, quantities that characterize the turbulence and the velocity and temperature fields. There is little effect of MHD forces on the thickness (or speed) of the flow in the case of Flinabe, but there was a significant effect on the heat transfer in the near surface. In general in the presence of a strong magnetic field, the turbulent eddies in the bulk of the fluid tend toward a 2-D state with circulation around the direction of the magnetic field and elongation in the direction of the field. Thus the turbulent structure is anisotropic, and near the free surface, there is also a damping of the turbulent transport. Also, the turbulence redistributes in the thin near-surface layer known as a blockage layer where blockage of turbulence, due to the capillary forces and the gravity force component normal to the free surface, results in suppression of the velocity pulsations normal to the free surface and some enhancement of the other two velocity components due to continuity. Such turbulence redistribution near the free surface reduces heat transfer rate (unless surface waves enhance fluid mixing within the blockage layer[46]). Thus, in these flows, one must characterize separately turbulence in the bulk fluid and turbulence near the free surface.

For fluids with poor thermal conductivity flowing in closed channel, the Reynolds Analogy is often assumed so that the turbulent Prandtl number[8] is approximately unity and does not vary across the layer. For liquid in the blockage layer near a free surface, the turbulence anisotropy at the surface can be characterized using the distribution for the turbulent Prandtl number evaluated for experimental data for subcritical flows (Froude number <1)[47]. In this distribution, the turbulent Prandtl number increases as the proximity to the free surface. In developing a solution for this problem, Smolentsev and collaborators incorporated Joule

[8] The turbulent Prandtl number is the ratio of eddy diffusivity for momentum to eddy diffusivity for heat.

dissipation from both velocity and electric field pulsations in the treatment of the dissipation term in the equation for turbulent kinetic energy and destruction term in the equation for the dissipation rate and utilized the "K-_" model to characterize the eddy diffusivity for momentum as well as effective thermal conductivity across the liquid layer. The model has been described in other publications, e.g., Ref. [45-47], and is summarized in a parallel paper in this journal[48].

5.2 Deflector Shape and Location

With an upstream deflector in the divertor, the next question is what determines its location. The somewhat extended discussion here on the location of the deflector also illustrates some basic issues of integrating the divertor into the first wall and blanket.

Fig. 10 is a map of flux surfaces from Rognlien, Rensink and Bulmer with two possible positions of a deflector (A and B) located at the outermost flux surface on this map (z7=7cm.). By making the arc of the deflector shorter or longer, the deflector can redirect the stream over a range of angles. In the figure, three such streams from deflector A cross the separatrix at points 1, 2, or 3. One stream from deflector B also crosses at intersection point 2, but at an angle of ~45°.

We can gain some understanding of the relative contributions of such factors as the angle of inclination between the flux surface and the divertor stream (target angle) and the effect of the change in flux expansion as one moves the strike point higher or lower in the divertor by considering a simple 1-D treatment for penetration of heat.

For a (semi-infinite) solid, the equation, T=q/k (□t/□), gives the temperature rise of the surface. In our case, the time t, is the transit time as the fluid crosses the strike point of the divertor. This time is inversely proportional to the flow velocity, v, and to the sine of the angle between the divertor surface and the flux surface. Let q be the parallel heat flux, i.e., the heat load that would be intercepted by a divertor target parallel to the toroidal vector and perpendicular to the flux surface. The equation blow gives the temperature rise of the surface and its dependence upon the angle and flux expansion.[9]

[9] A 1-D approximation is justified because the heat is penetrating into a surface layer less than 1mm thick and this distance is much smaller than the width over which the heat load is applied. The flux expansion factor is the ratio of the flux evaluated where the divertor flow intercepts the separatrix to the flux expansion at the location of a perpendicular target. The target angle is the poloidal angle between the stream and the separatrix.

$$T_{surf,rise} \approx \frac{q^*}{k}\sqrt{\frac{\alpha t}{\pi}} \quad \text{with} \quad t = \frac{L_0 flxp}{\sin(\theta) v} \quad \text{and} \quad q^* = q\frac{\sin(\theta)}{flxp}$$

$$= q\frac{\sin(\theta)}{flxp}\sqrt{\frac{1}{\pi k \rho C_p v}}\sqrt{\frac{L_0 flxp}{\sin(\theta)}}$$

$$T_{surf,rise} \approx q\sqrt{\frac{L_0}{\pi k \rho C_p}\frac{1}{v}}\sqrt{\frac{\sin(\theta)}{flxp}\frac{1}{k_{eff}}} \qquad (1)$$

This differs slightly from the direct dependence on sin(θ)/flxp for a solid target. The factor, (sin(θ)/flxp), is plotted in Fig. 11 as a function of the angle between the stream and the separatrix (z0 in Fig. 10). Position 1 has the largest flux expansion and lowest value of this factor at any specific angle down to the limit of about 40°, but this is the lowest target angle possible for Position 1 with the deflector still behind the Z7 flux surface. Position 3 can have the lowest factor overall because, even with less flux expansion, smaller target angle at that position reduces this heating factor to lower value.

The next consideration is to maximize the effective thermal conductivity (k_{eff}), which we do by placing the strike point as close as possible to the deflector. While the fluid passes the deflector, there is a strong shear layer that generates turbulence in the fluid adjacent to the deflector. When this fluid layer leaves the deflector, the turbulence begins to decay toward its steady state value in a free stream, and we have analyzed the importance of this effect.

In author Smolentsev's model of the decay of turbulence for Flibe (and we assume Flinabe will be the same), the turbulence built up in the layer adjacent to the deflector then drops rapidly over a length of roughly ~0.2m after the flow leaves the deflector. Figure 12 shows profiles of the turbulent viscosity versus the normalized distance from the back (flow substrate) to the free surface at several locations downstream from the deflector. A substrate must be present in this model[10] so there is a continuing source of drag to promote turbulence at the back surface; however, the right side of the plots gives some sense of how the turbulence decays from an initially higher value toward that of a developed free surface.

The greatest heat removal would occur if the peak heat flux were right at the exit of the deflector where the turbulence in the near surface is greatest. However, the turbulence is generally fairly high and the thermal penetration is good, which

[10] In the first zone in this model, the fluid passes along a solid "front" surface that represents the deflector. In the second zone, the front surface is free and the stream passes along a "back" surface while the free front surface receives a heat load with a profile appropriate for the divertor. (The back surface is required in this model but is not present in the ARIES-RS/CLIFF divertor design.) The fluid enters the deflector (initial boundary condition) with an initial temperature profile through its thickness established from the heating of the first wall. Due to the thermal mixing in the deflector region, the fluid leaves the deflector with all the fluid having the nearly the same average bulk temperature and with increased turbulence.

to some degree offsets the importance of the decay of turbulence in the near surface layer. Also, it is not practical to place the deflector close to the edge of the plasma.

Figure 13 shows the temperature profile along the divertor flow stream for (four) cases with the zone of high heat load beginning at 0.05, 0.10, 0.15 or 0.20m from the exit of the deflector. The peak surface temperature is progressively greater as the strike point is further from the exit of the deflector, and this rise is a combination of two effects.

First, the surface temperature rises due the background heat load of 3MW/m^2. When the strike point (high heat load) is further from the deflector, then surface temperature at the start of the high heat load region (T_{start}) is greater.

Second, due to the decay in turbulence, the increase in surface temperature, from T_{start} to T_{peak}, during just that portion when the surface is exposed to the higher heat flux is also greater as the distance of the strike point from the deflector increases. This incremental rise ranges from about 137°C in the first case to about 164°C in the fourth case.

Figure 13 shows T_{start} , the progressive change in the incremental temperature rise ($\Delta T_{rise} = T_{peak} - 136$) and the sum ($T_{sum} = T_{start} + \Delta T_{rise}$). The initial temperature rise from the "preheating" before the strike zone dominates for the cases shown, but the trend is that the contribution from the decay in the turbulence added by the deflector becomes increasingly important and the slope of the T_{sum} curve trends upward ($d^2T_{sum}/dx^2>0$). The implication of Smolentsev's model for our design is that the strike point should be within 0.15-0.2m along the flow from the exit of the deflector to take some advantage of the turbulence introduced in the deflector.

5.3 Concerns about "leading edges" and ripples

Another concern for heat removal in the divertor is the "leading edge" problem. Charged particles at the edge of a plasma travel parallel to (orbit around) the magnetic field lines and will deposit a tremendous heat load on any protrusion that has intercepted this particle flux. In a toroidally continuous smooth divertor, these particles (and their energy) spread evenly over the divertor surface. But if a toroidal opening exists, some particles diffuse radially outward and deposit on the edges of the opening. The local heat flux on these edges can be dramatically higher than the heat flux spread onto the smooth toroidal surface.

A commonly used technique for mitigating the "leading edge problem" is to make the plasma-facing surfaces near a leading edge recede gradually back to a distance where the heat flux onto the leading edge is low and the diffusing heat load spreads over this larger receding area. For example, one finds beveled tiles around openings for diagnostic ports in most large tokamaks. In the extreme use of this technique, one would design the face of the plasma-facing surface so that its shape would result in a uniform heat load (toroidally) along the strike point, and this heat load would be equal to the uniform heat load on a toroidally continuous surface divided by the fraction of (toroidal) area covered by the non-continuous surface. (This might work for a reactor in which the plasmas were

formed with the same shape, power, etc., but this approach is not necessarily applicable for the plasma facing components of an experimental device in which the plasma shape, power, etc. vary.)

For our divertor, we use the deflector (a) to separate the first wall flow into separate streams for each sector and (b) to produce streams in each sector that are slightly further away from the plasma at the sides (adjacent to the edges of the sector) than in the main portions of the streams. Stated another way, if one followed a trace along the strike point, the edges of the stream are at a position of slightly greater major radius than the portion in the center of the sector. Previous Figure 7 includes several 3-D drawings of the outer deflector that indicate features associated with some of the important functions are listed below.

- redirect first wall flow into exhaust duct (downward curvature)
- align flow (sharp fins in the upper portion)
- smooth surface of stream (smooth finish and close tolerance on deflector)
- edges of stream receding away from plasma (overall shape of deflector)
- flow or spray cools surface of duct (auxiliary stream from deflector)
- flow or spray cools exposed walls of divertor cassette (auxiliary stream)

Features have been included in the deflector to accomplish the functions above. However, as yet we do not have a computational fluid flow analyses to confirm that these features will produce the desired shape of the stream.

While we expect most of the objectives above to be straightforward in a detailed design and engineering of the divertor, the smoothness of the surface of the stream and the conformity to the ideal location cannot be confirmed without testing, or at least, detailed computational fluid dynamic calculations. This issue is discussed further in the Future R&D Section of another paper[26] in this journal.

6 Divertor Structure

The deflector is a prominent structure in the divertor and receives radiation from the main plasma and from the strongly radiating portion of the plasma near the separatrix. This radiation will also shine down into the exhaust duct and surrounding shield and, through the toroidal openings in the divertor stream, onto the walls of the divertor cassette behind (radially outward from) the divertor stream. In all these regions, we believe we can manage to cover the surfaces with some flow redirected from the main divertor stream. The heat fluxes will be somewhat lower and slower flow will be adequate. However, a detailed design of these streams has not been done.

The deflector is a relatively thin plate that can be adequately cooled by the flow of the Flinabe over that portion of the deflector that is wetted by the flow. For example, in an earlier design with a radiated heat load of 1.4MW/m^2, the plasma facing side of a 5mm deflector plate made of 316SS would be about 500°C hotter than the wetted surface. The temperature difference for an advanced ferritic steel (AFS) plate, with a (higher) thermal conductivity of about 33W/m-°C would

be about 212°C. However, with the highly radiating regions near the separatrix, the heat load onto the deflector is higher, (~3MW/m^2). In this case the difference in temperature is 455°C for a 5mm-thick AFS deflector and a material with higher thermal conductivity is needed. A 4.5mm-thick copper deflector would have a temperature differential of only 34°C and 0.5mm-thick cladding of AFS on each side would add 45°C twice for a total of 124°C, which is acceptable.

While most of the area on the back of the deflector is in contact with the flowing Flinabe, there must be a lip at the upstream entrance to catch any waves. This lip receives the same heat flux as the rest of the deflector but must conduct this heat internally down to the area that is cooled by the Flinabe. So the hottest spot on the deflector will be at the top of this lip.

An initial thermal analysis of the deflector indicated that (a) the deflector should be made of a good thermal conductor and (b) the lip would need to be thicker than the rest of the deflector to increase its internal thermal conductance. Several (PATRAN/ABAQUS) finite element models with various versions of a 100mm-long “thick lip” were created. The material is copper with a 0.5mm cladding of an advanced ferritic steel. This model uses values of the heat transfer coefficient along the deflector from the case by Smolentsev noted above. For these cases with a long (100mm) lip at a shallow angle with the fluid, the peak temperature at the end of the lip was reduced as the configuration revised from much higher temperatures to about 900°C, as shown in Fig. 14. If such a long lip is needed (as might be shown by future analyses and experiments on the waviness of the first wall flow), then we could use a design with cooling channels inside the lip and auxiliary cooling by Flinabe. Such a design is quite possible and would be accomplished by placing cooling channels in the deflector lip and connecting cooling passages in the body of the deflector and its support structure. Conversely, a shorter lip might not require such cooling. But such design work as well as the experiments and analysis on flows around penetrations remains as future work.

Adequate cooling must also be provided for the portions of the structure around the exhaust duct that are not shielded by the fast flowing fluid in the divertor. Figure 15 shows a view downward into the divertor where one may see the regions of the upper shield that would be exposed via line-of-sight to radiation from the plasma (if these surfaces were not covered by flowing Flinabe). There are heat loads from radiation onto portions of the shield. The shield behind the deflected stream in the outer divertor receives radiation through the toroidal separations in the flow curtain over the sector joints. And some portions around the edges of the exhaust ducts are not directly covered or shielded by the fast flowing inboard or outboard coolant. The likely need for some supplemental cooling at these sites is recognized and work is in progress.

7 Divertor – A Completely New approach

A new and radical innovation in power handling was introduced in APEX by author Kotschenreuther.[49] In this scheme, depicted in Fig. 16, small coils alter the flux surfaces at the edge of the plasma and introduce magnetic channels

through which the flux surfaces pass outside the toroidal field coils where there is much greater area available to disperse the energy, a very low neutron flux, and enormously greater access for pumping and maintenance.

Certainly the basic concept of a “bundle” divertor has been advanced previously, for example in an early design in the US in the late 1970’s for a “next step” experiment called the Fusion Engineering Device. The unique feature of Kotschenreuther’s concept is that the extraction of field lines is accomplished with many small coils so that there is not a large or asymmetric perturbation in the overall shape of the torus. The field lines exit the TF coils as relatively narrow jets and the scheme does not introduce unacceptable magnetic field ripple at the plasma surface. Also, the concept enables new regimes of profoundly reduced recycling, with the prospect of greatly improved confinement.

The concept uses conventional PF coils to bring the separatrix to the TF coils. Additional non-axi-symmetric coils must be added near the TF coils to redirect field lines around the TF coils. Several configurations have been explored, which are far superior to bundle divertor concepts, in that they require less current and produce far less field ripple at the plasma surface.

Calculations have been performed using a free boundary axi-symmetric MHD equilibrium code developed at the Institute for Fusion Studies (University of Texas at Austin). The code includes features novel to this problem, such as (1) constraints on the field line path of the separatrix well outside the plasma, and (2) the axi-symmetric component of the fields of the non-axi-symmetric redirection coils must be included. This is coupled to a three dimensional field line tracing code.

As an example, we consider a case with parameters very similar to the ARIES-AT design for a 1 GW electric power reactor. Configurations have been found with field ripple at the plasma surface less than 0.6 %. The entire scrape-off layer region is extracted (within 5 cm of the separatrix) and misses realistic sized TF coils by about 0.4m on the outboard side and 0.2m on the inboard side.

One feasible embodiment of the divertor would be to have each jet enclosed in a cylindrical vacuum chamber which is an extension of the main vacuum chamber, and connected to it through a relatively narrow throat. The cylinders are easily accessible for maintenance. With the assumptions of no radiation from the main chamber into a cylinder, the heat load on the surface of the cylinder can be reduced to ~2 MW/m^2 with a detached plasma in the cylinder or ~5 MW/m^2 with an attached plasma. Similar results are possible for low aspect ratio cases.

8 Closing Remarks and Acknowledgements

Certainly there are many issues associated with free surface liquid divertors. Another paper[26] in this issue of Fusion Engineering and Design describes the design for a fusion chamber with flowing Flinabe walls, reviews design work with liquid metal walls and presents a summary of R&D issues within the context of the overall chamber design activity. We refer the reader to the summary of R&D issues in that article rather than repeat them here. Certainly, detailed

computational fluid dynamics analyses and testing to validate the analyses would be useful in further developing the design of the Flinabe flow for the divertor in our design.

We again emphasize that the MHD effects on flow must be evaluated to give a realistic rendering of liquid metal flow streams in the chamber. As we continue to evaluate possibilities for a liquid surface divertor, there is ongoing development by the APEX Team of the modeling tools needed for the evaluation of these complicated liquid metal MHD-controlled flows. Readers interested in that ongoing development may wish see the papers by Morley et al. and by Smolentsev et al. elsewhere in this journal[48,50] and to check the APEX website[1] for other information and references.

A goal of the APEX and ALPS Programs in the US is to investigate the potential for the use of free liquid surfaces in fusion chamber technology. And to do so with a sufficient level of effort that the design issues can be resolved and an accurate assessment of this potential can be understood. In this work, we are supported by the APEX and ALPS Teams and a significant programmatic commitment by the Department of Energy's US Fusion Energy Science Program has enabled us to utilize diverse expertise in plasma edge modeling, advanced mechanical and systems design, and heat transfer. Although still in the early phase of developing liquid surface concepts, we have made significant progress in identifying useful coolants, divertor geometries and plasma edge conditions. The work of two authors (TDR and MER) was performed under the auspices of the U.S. Department of Energy by contractW-7405-Eng-48 at the University of California Lawrence Livermore National Laboratory.

References

[1] M. Abdou et al., Exploring novel high power density concepts for attractive fusion systems, Fus. Eng. & Des. 45 (1999) 145; many APEX presentations are available on <http://www.fusion.ucla.edu/APEX/>

[2] R. Mattas and ALPS Team, ALPS - Advanced Limiter-Divertor Plasma Facing Systems, Fus. Eng. & Des. 49-50 (2000) 127; see the ALPS website <http://fusion.anl.gov/ALPS_Info_Center/calls.html>

[3] J.C.R. Hunt, Hancox, The use of liquid lithium as a coolant in a toroidal fusion reactor, Part 1: calculation of the pumping power, CLRM-115, Culham Laboratory (1971)

[4] M.A. Hoffman, Magnetic Field Effects on the Heat Transfer of Potential Fusion Reactor Coolants, UCRL-73993 (1972)

[5] B. Badger, *UWMAK-I, A Wisconsin Toroidal Fusion Reactor Design*, University of Wisconsin, UWFDM-68, 1973

[6] L. Golubchikov, Development of a Liquid-Metal Fusion-Reactor Divertor with a Capillary-Pore System, JNM, 237 (1976) 667-672

[7] J.H. Pitts, A Consistent HYLIFE Wall Design that Withstands Transient Loading Conditions, 4th ANS Topical Mtg. On the Technology of Controlled Nuclear Fusion, King of Prussia, PA, Oct. 14-17, 1980

[8] E. Muraviev, Contact Devices for Divertor and Limiter Systems of Tokamak Reactors. I. Devices with LM Working Surface, Voprosy Atomnoi Nauki I Tekhniki, Ser. Termoyaderniy Sintez, 2, (1980) 57-64

[9] W. Wells, A System For Handling Divertor Ion and Energy Flux Based on a Lithium Droplet Cloud, Nuclear Technology/Fusion,1, (1981) 120

[10] V. Baranov, Liquid Metal Film Flow for Fusion Application, 7th Beer Sheva International Seminar on Liquid Metal Magnetohydrodynamics, 1983

[11] A. Bond, A Liquid Metal Protected Divertor for a Demo Reactor, 13th Symposium on Fusion Technology, Varese, Italy, (1984) 1225

[12] B. Karasev, LM Contact Divertor for INTOR Tokamak Reactor, 4th All-Union Conf. on Engineering Problems of Fusion Reactors, Leningrad, (1988) 225-256

[13] V. Vodyanyuk, 'Liquid Metal Tokamak Limiter - Problem Definition and First Results, Plasma Physics, 14, (1988) 628

[14] I. Kirillov, Alternate Concepts of the Divertor Targets Working Materials to the ITER, October 1990, ITER-IL-PC-8-0-18

[15] C. Liao, A Feasibility Assessment of Liquid-Metal Divertors, Fusion Technology, 21, (1992)1845-1851

[16] S. Mirnov, Liquid-Metal Tokamak Divertors, JNM, 196, (1992) 45-49

[17] V. Chuyanov, Advanced Divertor Plates System Development Proposal, ITER EDA Memo, 1994

[18] E. Muraviev, Liquid-Metal-Cooled Divertor for ARIES, Fusion Engineering and Design, 29 (1995) 98-104

[19] E. Muraviev, Open Surface MHD Flow of Liquid Metal Coolant in a Rotating Divertor Target of a Tokamak Fusion Reactor, Magnetohydrodynamics, 31 (1995) 306

[20] V. Pistunovich, "Research of the Capillary Structure Heat Removal Efficiency Under Divertor Conditions, JNM, 237, (1996) 650-654

[21] V. Lazarev et al., Compatibility of the lithium capillary limiter with plasma in T-11M, ECA, 23J (1999), 845-848

[22] V.A. Evtikhin et al., Energy removal and MHD performance of lithium capillary-pore systems for divertor target application, FED, 49 (2000) 195-199

[23] M.A. Mahdavi, M. Schaffer, Heat Removal with a Liquid Pellet Curtain (paper), *Innovative Confinement Concepts Workshop* held at Princeton Plasma Physics Laboratory, April 1998.

[24] M.A. Tillack et al., Engineering Design of the ARIES-RS Power Plant, Fus. Eng. & Des. 41 (1998) 491; also <http://aries.ucsd.edu/PUBLIC/ariesrs.html>

[25] C.P.C Wong, et al., ARIES Divertor System - Selection and Analysis, FED 38 (1997) 115

[26] R.E. Nygren, et. al., A fusion reactor design with a liquid first wall and divertor, elsewhere in this journal

[27] T.D. Rognlien, M.E. Rensink, Interactions between liquid-wall vapor and edge plasmas, JNM 290-293 (2001) 312-316

[28] R. Bastasz and W. Eckstein, Plasma-Surface Interactions on Liquids, JNM

290-293 (2001) 19-24
[29] N. Morley et al., Modeling for liquid metal free surface MHD flow for fusion liquid walls elsewhere in this journal; see also, N. B. Morley, S. Smolentsev and D. Gao, Modeling infinite/axisymmetric liquid metal magnetohydrodynamic free surface flows, FED 63-64 (2002) 343-351
[30] T.D. Rognlien and M.E. Rensink, Edge-plasma properties in liquid-wall environments, 8th Int. Workshop on Edge Plasma Theory in Fusion Devices, Helsinki, Finland, Sept. 10-12, 2001

[31] J.N. Brooks, D. Naujoks, Sheath superheat transmission due to redeposition of thermally emitted material, Physics of Plasmas 7 (2000) 2565
[32] D. Naujoks, J.N. Brooks, Combined sheath and thermal analysis of overheated surfaces in fusion devices, JNM 290-293(2001) 1123
[33] J.N. Brooks, T.D. Rognlien, D.N. Ruzic and J.P. Allain, Erosion/redeposition of lithium-based liquid surface divertors, JNM 290-293(2001) 185
[34] J.N. Brooks, Modeling of sputtering erosion/redeposition - status and implications for fusion design, FED, 60 #4 (July 2002) 515-526
[35] R. Doerner, M.J. Baldwin, M.J., R.W. Conn, A.A. Grossman, S.C. Luckhardt, R. Seraydarian, G.R. Tynan, D.G. Whyte, Measurements of erosion mechanisms from solid and liquid materials in PISCES-B, JNM 290-293 (2001) 166-172; also M.J. Baldwin, R. Doerner, S.C. Luckhardt, R. Seraydarian, D.G. Whyte, R.W. Conn, Plasma interaction with liquid lithium: Measurements of retention and erosion, FED 61-62 (2002) 231
[36] J.P. Allain, M.D. Coventry, D.N. Ruzic, Temperature dependence of liquid-lithium sputtering from oblique 700 eV He ions, JNM 313 (Mar 2003) 641-645
[37] J.P. Allain, D.N. Ruzic, M.R. Hendricks, D, He and Li sputtering of liquid eutectic Sn-Li, JNM 290 (March 2001) p33-37, and J.P. Allain, D.N. Ruzic, M.R. Hendricks, Measurements and modeling of D, He and Li sputtering of liquid lithium, JNM 290 (March 2001) 180-184
[38] M.J. Baldwin, R. Doerner, S.C. Luckhardt, R.W. Conn, Deuterium retention in liquid lithium, Nucl. Fusion, 42 (2002) p1318-1323; and M.J. Baldwin, R. Doerner, R. Causey, S.C. Luckhardt, R.W. Conn, Recombination of deuterium atoms on the surface of molten Li–LiD, JNM 306 (2002) 15-20
[39] R. Bastasz, Surface Studies of Liquid Metals and Alloys, Proceedings of the Int. Symp. Material Chemistry in the Nuclear Environment (2002) in press
[40] K. Shimada, T. Tanabe, R. Causey, T. Venhaus, and K. Okuno, Hydrogen recycling study by Balmer lines emissions in linear plasma machine TPE, J. Nucl. Mater. 290-293 (2001) 479
[41] J.P. Allain, M. Nieto, M.D. Coventry, M.J. Neumann, E.Vargas-Lopez, D.N. Ruzic, FLIRE - flowing liquid surface retention experiment, design and testing, FED 61-62, (Nov 2002) 245-250; also M. Nieto, D.N. Ruzic, J.P. Allain, M.D. Coventry, E.Vargas-Lopez, Helium retention and diffusivity in flowing liquid lithium, JNM 313 (Mar 2003) 646-650
[42] See for example, A. Hassenein, Prediction of material erosion and lifetime during major plasma instabilities in tokamak devices, FED, 60 #4 (July 2002)

527-546

[43] M.A. Ulrickson, Part 4, Section 6 Heat Flux Limits for Flowing Liquids, in ALPS Report, August 2001, 160 see ALPS website in Ref. 2

[44] R.E. Nygren, Part 4, Section 7 Notes on the thermal Properties of Sn, in ALPS Report, August 2001, 162, see ALPS website, in Ref. 2

[45] S.Smolentsev, M.Abdou, N.Morley, A.Ying, T.Kunugi, Application of the K-epsilon model to open channel flows in a magnetic field, International Journal of Engineering Science 40 (2002) 693-711

[46] B.Freeze, S.Smolentsev, N.Morley, M.Abdou, Characterization of the Effect of Froude Number on Surface Waves and Heat Transfer in Inclined Turbulent Open Channel Water Flows, Int. J. of Heat and Mass Transfer 46 (2003) 3765-3775.

[47] H.Ueda, R.Moller, S.Komori, T.Mizushina, Eddy diffusivity near the free surface of open channel flow, Int. J. Heat Mass Transfer 20 (1977) 1127

[48] S. Smolentsev et al., Thermofluid modeling and experiments for free surface flows of low-conductivity fluid in fusion systems, elsewhere in this journal

[49] M. Kotschenreuther et. al, Improved Plasma Performance Through Innovative Boundary Control Techniques, 19th IAEA Fusion Energy Conference (Proc. 19th Int. Conf. Lyon, 2002), IC/P-04

[50] N. Morley et al., Modeling for liquid metal free surface MHD flow for fusion liquid walls, elsewhere in this journal; also N. B. Morley, S. Smolentsev and D. Gao, Modeling infinite/axisymmetric liquid metal magnetohydrodynamic free surface flows, FED 63-64 (2002) 343-351

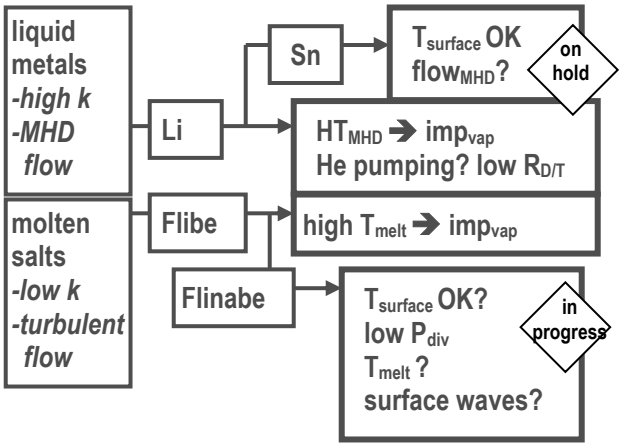

Figure 1. Summary of research paths on liquid surface divertors

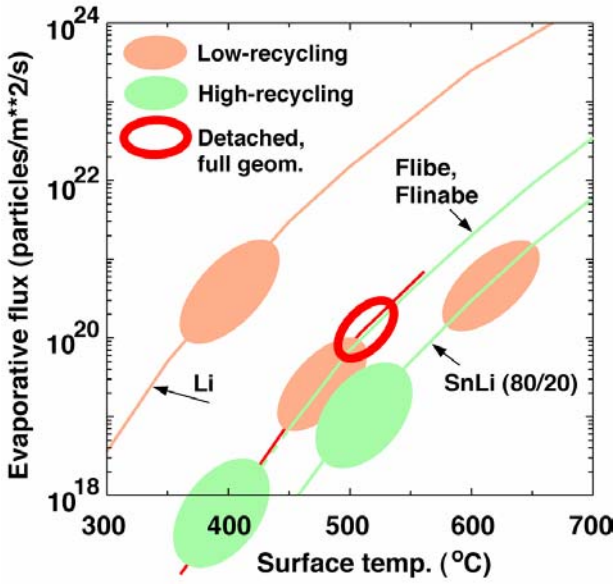

Figure 2. Operating temperature limits based on allowable limits for plasma impurities and modeling with the UEDGE Code.

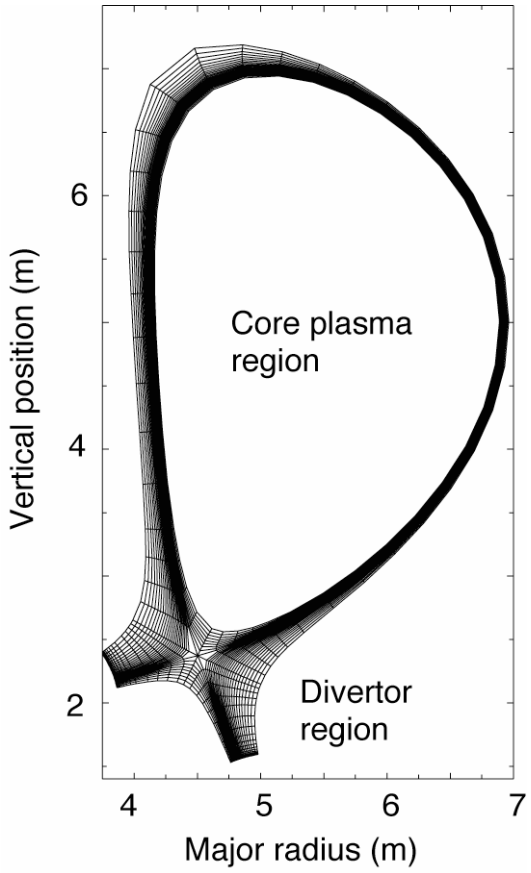

Figure 3. Mesh for UEDGE 2-D model of APEX/ARIES plasma edge

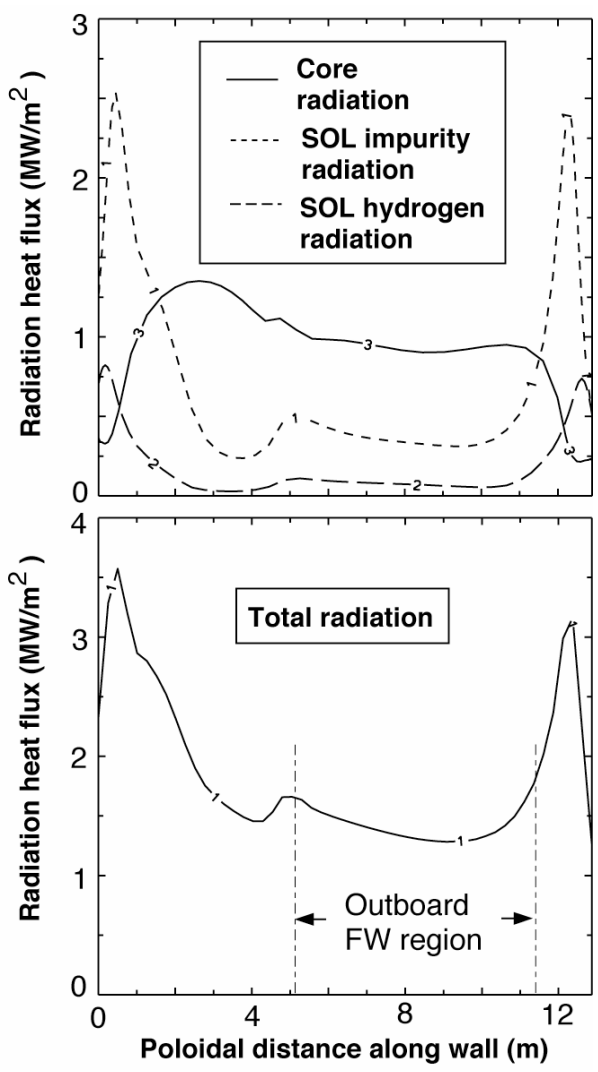

Figure 4. Radiated heat flux vs. distance around the chamber from UEDGE model.

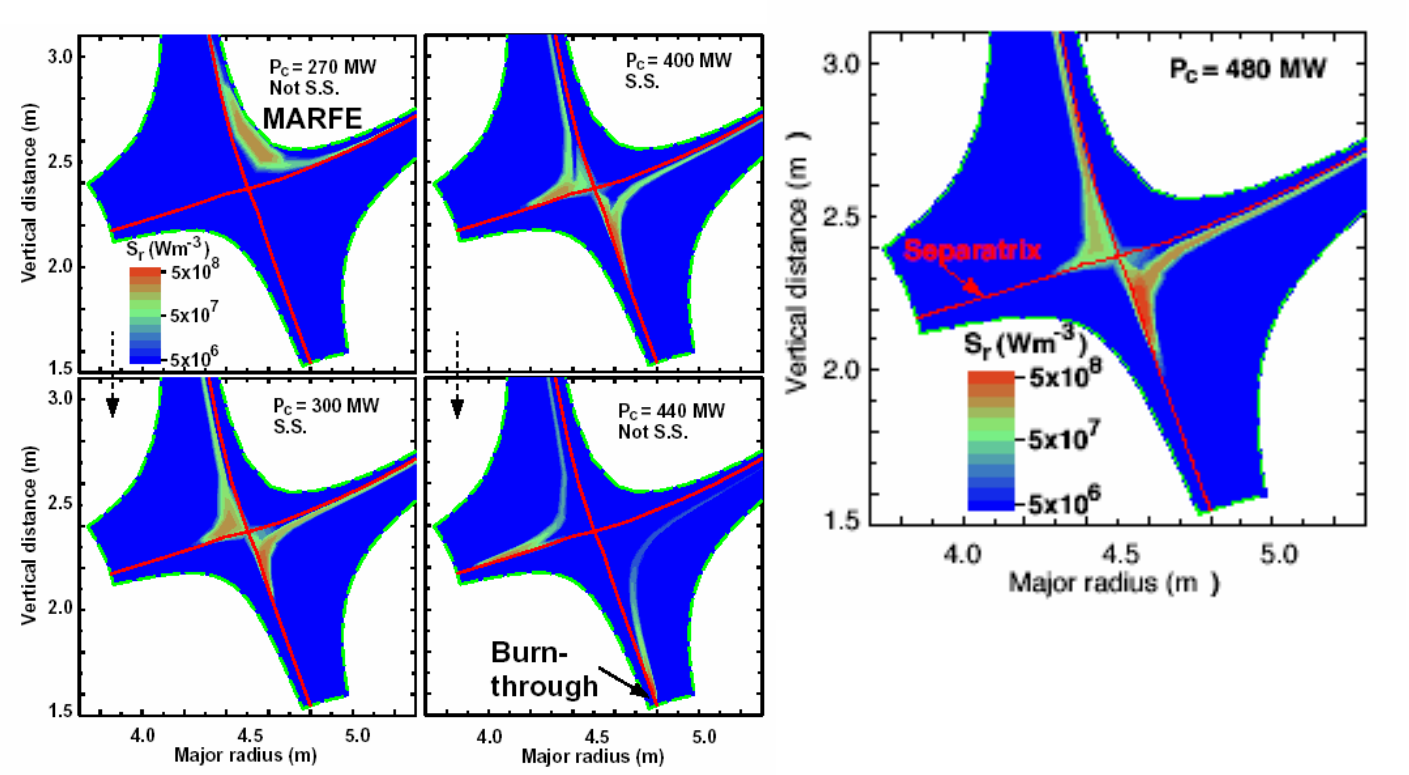

Figure 5. UEDGE "maps" of fluorine radiation. See text for explanation.

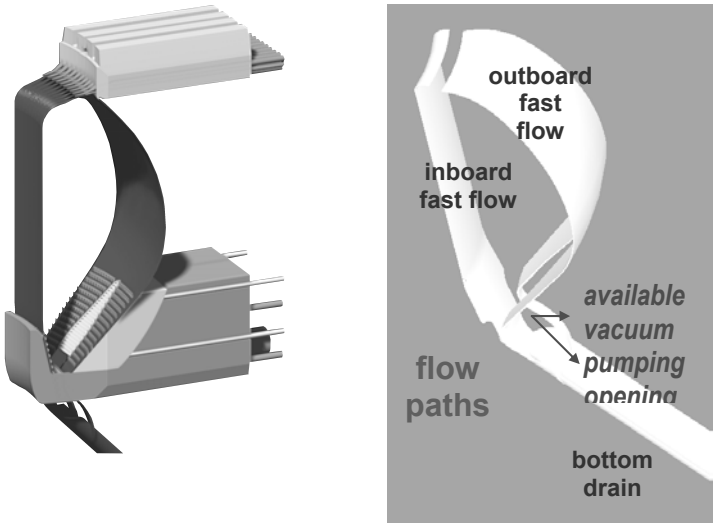

Figure 6. Earlier configuration of outboard divertor with large port for RF lancher, division of the flow into two streams and a downstream deflector.

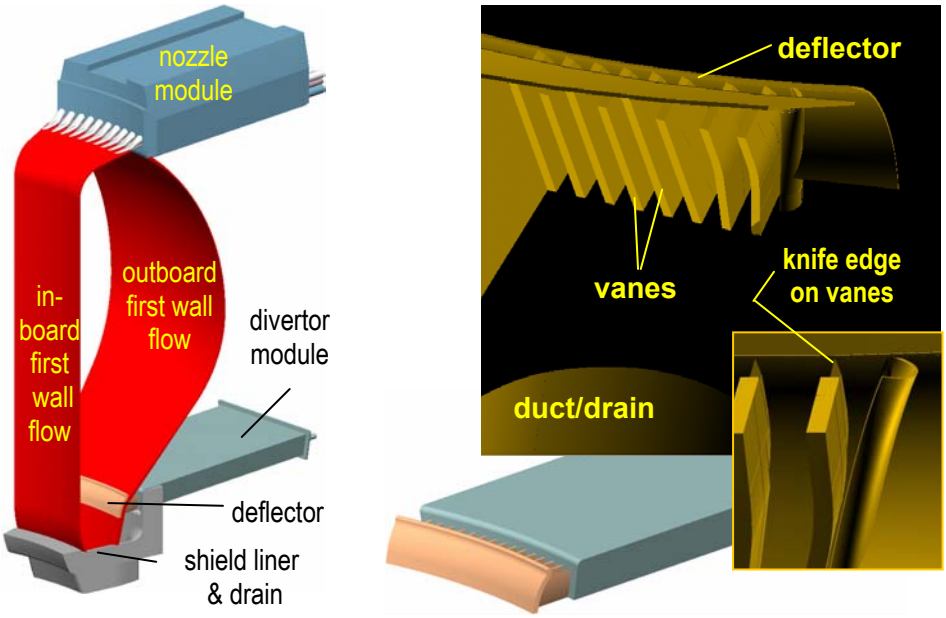

Figure 7. New configuration of ARIES/CLIFF outer divertor with deflector upstream of strike point.

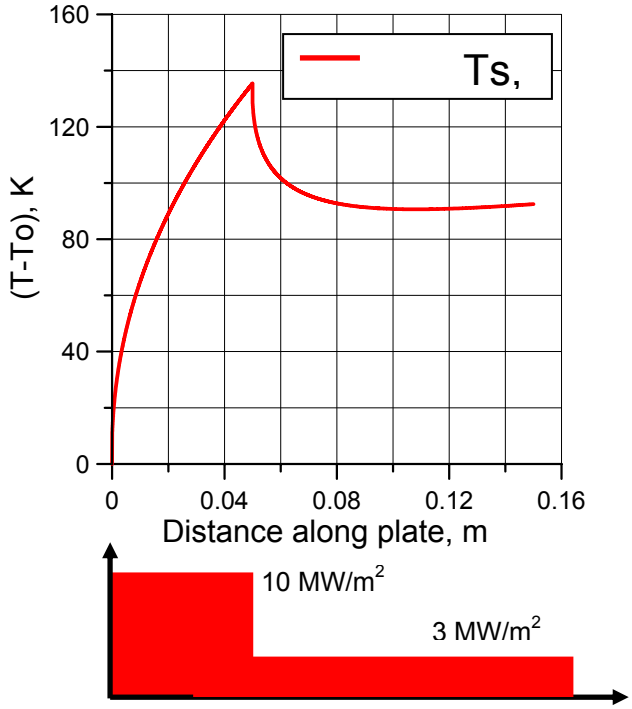

Figure 9. Temperature rise of Flinabe in divertor vs. distance along flow.

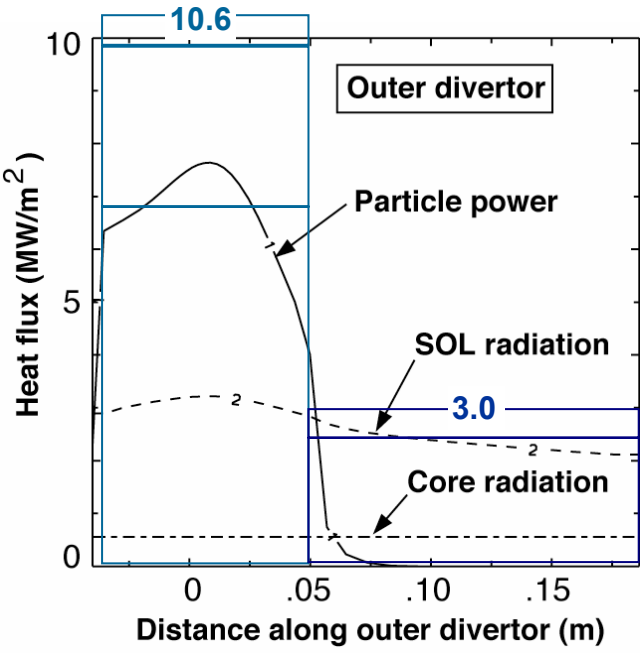

Figure 8. Heat load profiles for the divertor from UEDGE and average values for peak and background.

Figure 10. Portion of a flux map for ARIES-RS with a single null divertor (by Bulmer and Roglien, LLNL) overlaid with positions studied for a free surface divertor stream.

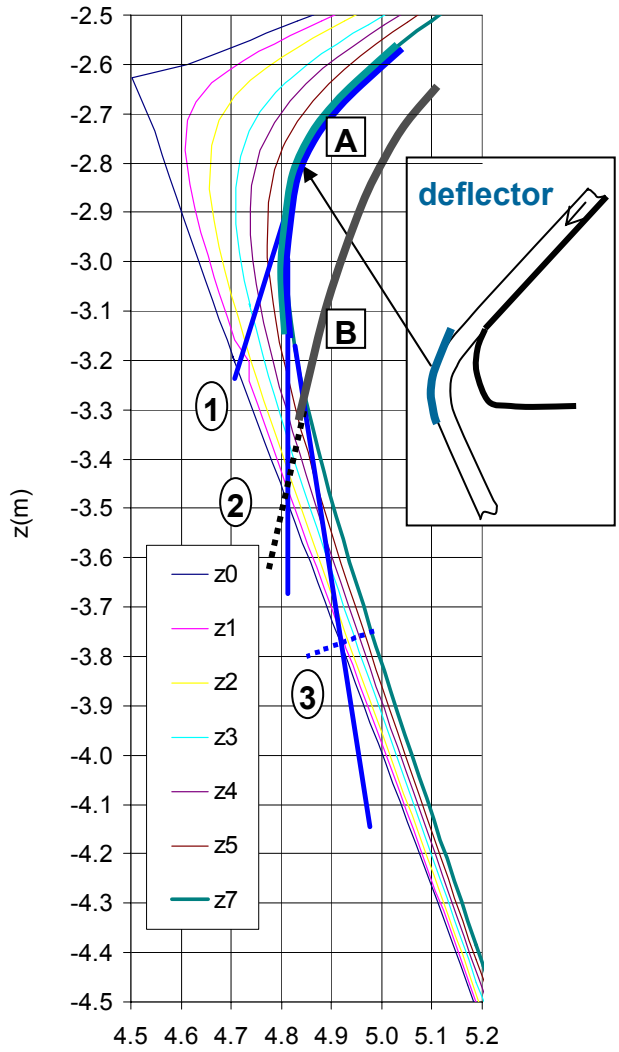

Figure 11. Dependence of temperature rise of the divertor surface (proportional to $\sqrt{[\sin(\theta)/\text{flxp}]}$ on the flux expansion (location) and target angle.

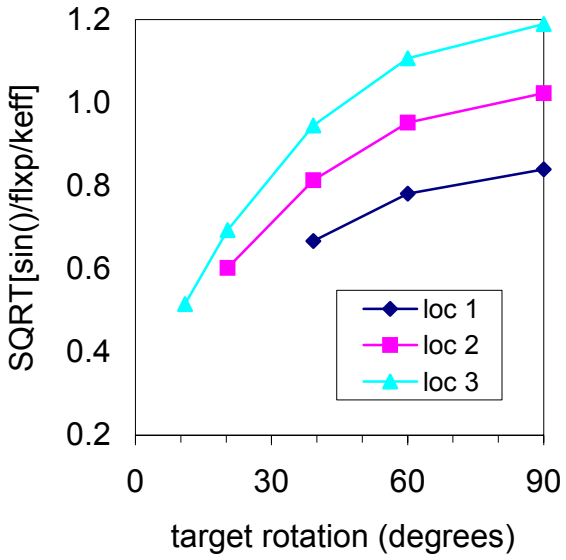

Figure 12. Profiles of turbulent viscosity vs. normalized distance from back surface of flow at several distances downstream from exit of deflector.

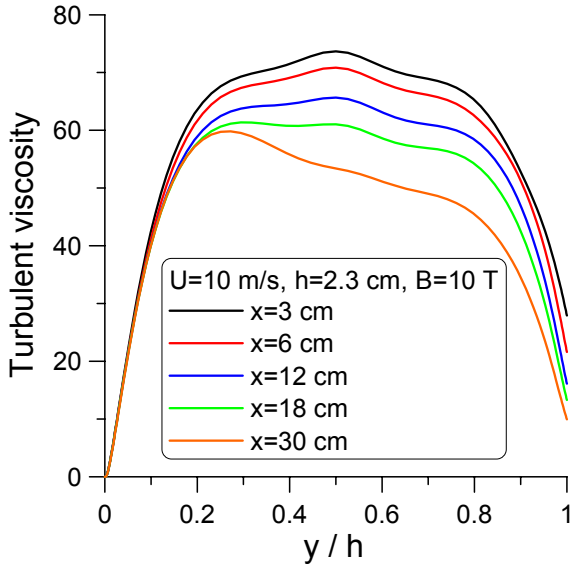

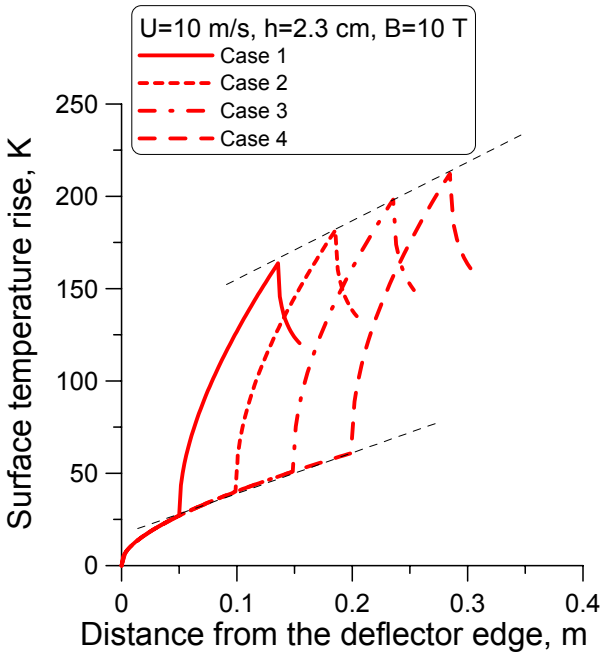

Figure 13. Surface temperature vs. distance from exit of deflector along divertor flow for four cases with the peak divertor heat flux located at 5, 10, 15 or 20 cm downstream from the deflector.

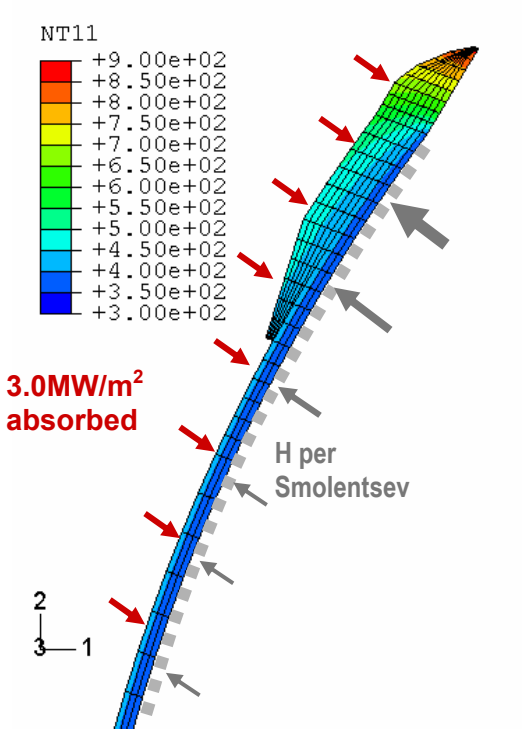

Figure 14. Thermal analysis of deflector from PATRAN/ABAQUS model and heat transfer coefficients for Flinabe taken from Smolentsev's model.

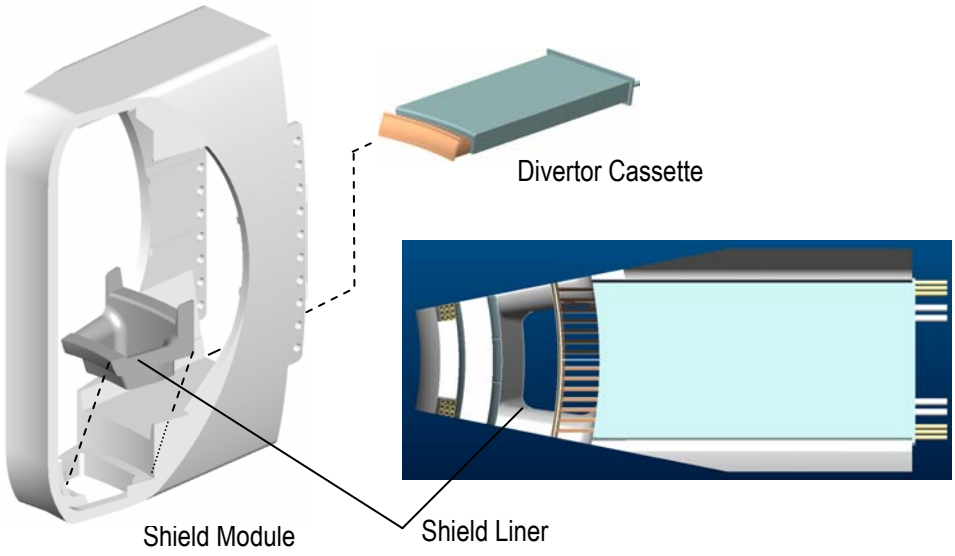

Figure 15. Surface temperature versus position along the divertor flow stream downstream of the deflector.

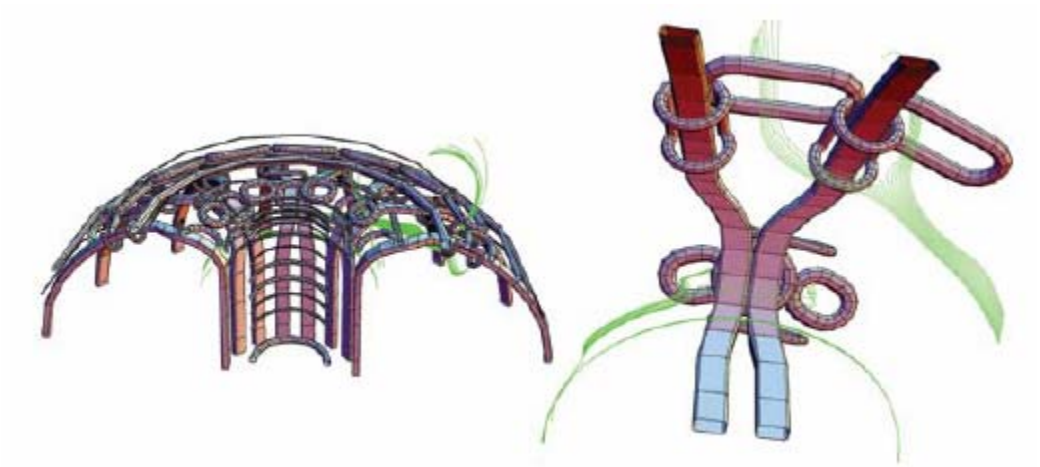

Figure 16. A completely new concept by Kotschenreuther of U. Texas, Austin for a divertor uses small coils to route some flux surface (shown here) outside the toroidal field coils where the surface for heat removal can be expanded.